Inorganic Chemistry

Article

pubs.acs.org/IC

Tuning Cobalt(III) Schiff Base Complexes as Activated Protein Inhibitors

Marie C. Heffern,[†] Viktorie Reichova,[†] Joseph L. Coomes, Allison S. Harney, Elizabeth A. Bajema, and Thomas J. Meade*

Departments of Chemistry, Molecular Biosciences, Neurobiology, Biomedical Engineering, and Radiology, Northwestern University, Evanston, Illinois 60208-3113, United States

Supporting Information

ABSTRACT: Cobalt(III) Schiff base complexes ($[Co(acacen)(L)_2]^+$, where L = NH_3) inhibit histidine-containing proteins through dissociative exchange of the labile axial ligands (L). This work investigates axial ligand exchange dynamics of $[Co(acacen)(L)_2]^+$ complexes toward the development of protein inhibitors that are activated by external triggers such as light irradiation. We sought to investigate ligand exchange dynamics to design a Co(III) complex that is substitutionally inert under normal physiological conditions for selective activation. Fluorescent imidazoles (C3Im) were prepared as axial ligands in $[Co(acacen)(L)_2]^+$ to produce complexes (CoC3Im) that could report on ligand exchange and, thus, complex stability. These fluorescent imidazole reporters guided the design of a new dinuclear Co(III) Schiff base complex containing bridging diimidazole ligands, which exhibits enhanced stability to ligand exchange with competing imidazoles and to hydrolysis within a biologically relevant pH range. These studies inform the design of biocompatible Co(III) Schiff base complexes that can be selectively activated for protein inhibition with spatial and temporal specificity.

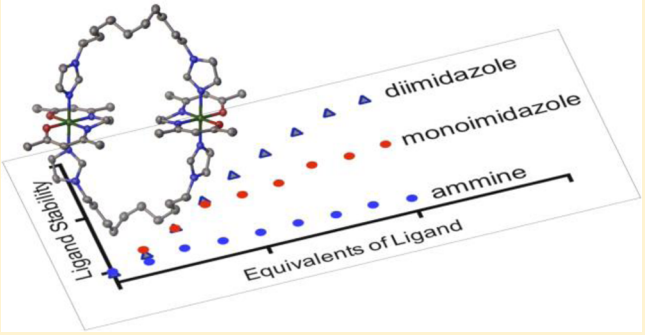

INTRODUCTION

Since the serendipitous discovery of the anticancer metallodrug cisplatin, the field of bioinorganic chemistry has seen significant advances in the development and rational design of transition-metal complexes for therapeutic applications. While DNA is considered the classical target of many metal complexes, researchers have discovered proteins as possible targets of bioactive inorganic molecules.[1−6] Cobalt(III) Schiff base complexes bearing labile axial ligands ($[Co(acacen)(L)_2]^+$, where L = NH_3, termed $CoNH_3$ in Figure 1) inhibit histidine-containing proteins and enzymes including zinc finger transcription factors (TFs) and metalloendopeptidases.[7−12] Protein inhibition occurs through a dissociative exchange of the axial ligands for the imidazole nitrogens of histidine residues (Figure 1A).[11,13−16] Binding of the complexes to histidine residues in structural or catalytic sites inhibits protein function. Target selectivity has been achieved through conjugation of the cobalt complexes to peptides and oligonucleotides with high affinity and selectivity for the proteins of interest.[7,8,10,17] The potential of these conjugates has been demonstrated in the specific inhibition of the Snail and Gli family of zinc finger transcription factors associated with cancer progression.[7,8,10]

In addition to the targeting moiety, the protein inhibitory activity of Co(III) Schiff base complexes may be controlled by tuning ligand dissociation. In this scenario, the Co(III) complex is designed to be substitutionally inert to axial ligand dissociation, and thus inactive as a protein inhibitor. In the presence of an external trigger, the coordination bond between the Co(III) center and the axial ligand is weakened, facilitating ligand exchange and protein inhibition. Such a pro-drug strategy would provide spatial and temporal specificity for improved efficacy and selectivity of the complex.

The feasibility of this strategy was demonstrated via a nanoparticle approach using redox activation of CoIm (the $[Co(acacacen)(L)_2]^+$ complex, where L = imidazole; see Figure 1) by photoinduced electron transfer (PET) from PbS quantum dots.[18] Relative to $CoNH_3$, CoIm exhibits higher stability to ligand exchange in the presence of a competing N-heterocycle and histidine mimic, 4MeIm.[15,16] Irradiation of the quantum dots reduced the Co(III) center to Co(II) by PET into the d_z^2 orbital while weakening the axial ligand bond to facilitate ligand dissociation. Subsequent oxidation to Co(III) through charge recombination produced the protein inhibitor. To improve the biocompatibility of the system, the redox activation strategy was translated to a molecular system whereupon a Ru(II) bipyridyl complex was covalently attached to CoIm.[19] Irradiation of the complexes at 455 nm light through PET resulted in a 5-fold increase in protein inhibition of the histidine-containing enzyme, α-thrombin, demonstrating

Received: June 25, 2015
Published: September 2, 2015

DOI: 10.1021/acs.inorgchem.5b01415
Inorg. Chem. 2015, 54, 9066−9074

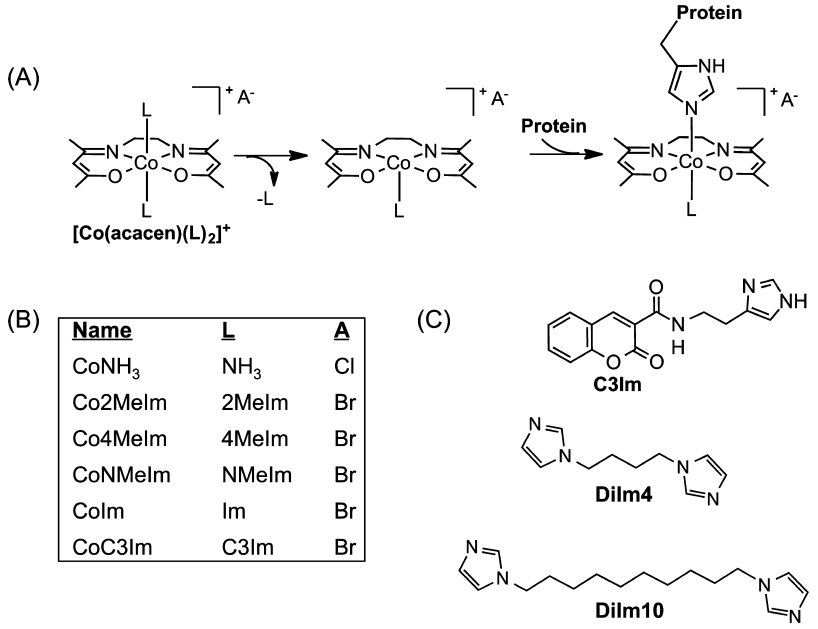

Name	L	A
$CoNH_3$	NH_3	Cl
Co2MeIm	2MeIm	Br
Co4MeIm	4MeIm	Br
CoNMeIm	NMeIm	Br
CoIm	Im	Br
CoC3Im	C3Im	Br

Figure 1. (A) Proposed mechanism of protein inhibition of Co(III) Schiff base complexes, $[Co(acacen)(L)_2]^+$. $[Co(acacen)(L)_2]^+$ complexes contain Co(III) metal centers stabilized by a tetradentate acetylacetone ethylenediimine (acacen) ligand. When the axial ligands are labile ammines ($CoNH_3$), the complex undergoes dissociative ligand exchange, allowing coordination of imidazole side chains of His residues. Incorporation of imidazole-containing ligands (Im, 4MeIm, and NMeIm) stabilizes the complex to ligand exchange.[12,15,16] When the axial ligands are 2MeIm, steric crowding of the methyl group results in a $[Co(acacen)(L)_2]^+$ complex that is substitutionally labile in aqueous environments with biological activity similar to that of $CoNH_3$.[12] (B) Naming of $[Co(acacen)(L)_2]^+$ complexes. (C) Structure of new imidazole ligands: fluorescent imidazole, C3Im; diimidazole ligands, DiIm4 and DiIm10. DiIm10 coordinates at the axial positions of $[Co(acacen)(L)_2]^+$ complexes to produce a stable dinuclear complex bridged by the diimidazole ligand.

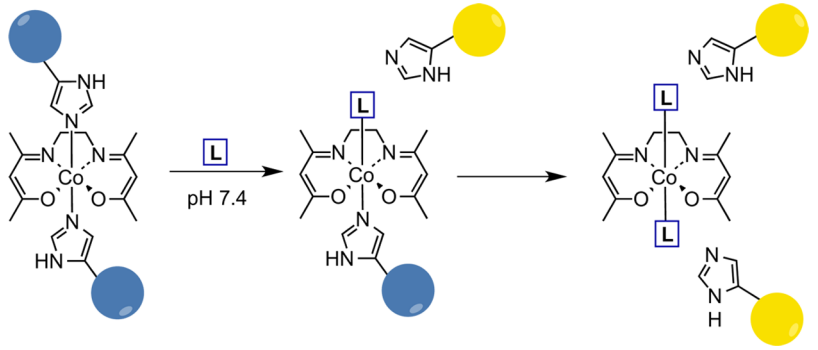

Figure 2. Mechanism by which fluorescently labeled imidazoles report on ligand exchange of $[Co(acacen)(L)_2]^+$ complexes. The fluorescent imidazole (C3Im) is quenched through Co(III) coordination (blue circles). Displacement of C3Im restores fluorescence (yellow circles), and the changes in emission intensity can be monitored to analyze ligand exchange dynamics.

the promise of light-activatable Co(III) Schiff base complexes for pro-drug strategies.[19]

Although CoIm exhibits increased stability prior to redox activation, compared to $CoNH_3$, ligand exchange and enzyme inhibition is still observed prior to light exposure. In the presence of a competing 4MeIm ligand at neutral pH, 50% of the Co(III)-Im bonds are exchanged for Co(III)-4MeIm bonds. In addition, while enzyme inhibition of α-thrombin by CoIm when conjugated to the Ru(III) bipyridine complexes is more pronounced upon light activation (k_{app} = 3.8 × 10^{-4} s^{-1} for enzyme inhibition), a degree of enzyme inhibition is still observed in the dark state (k_{app} = 6.8 × 10^{-5} s^{-1}).[19] This suggests that, in biological environments, the coordinative stability of CoIm may not be sufficient to preclude off-target binding to histidine-containing proteins prior to applying an external trigger. A more complete understanding of axial ligand dynamics is required to design complexes that are substitutionally inert under normal physiological conditions for selective activation with a specific stimulus.

In order to improve the design of activatable cobalt complexes, this study was conducted, with the objective being to develop a Co(III) Schiff base complex with enhanced stability that can serve as a platform for selectively activatable derivatives of the complex. To investigate ligand exchange in a facile manner, a fluorescently labeled imidazole ligand was developed (C3Im in Figure 1C). Fluorescent ligands have been previously implemented in Co(III) complexes to monitor ligand exchange under biological conditions.[20−22] In these examples, coumarin cores are attached to "receptor" moieties that coordinate to the Co(III) complexes of interest.[20−22] Fluorescence of this complex is quenched by Co(III) coordination but is restored upon axial ligand dissociation

DOI: 10.1021/acs.inorgchem.5b01415
Inorg. Chem. 2015, 54, 9066−9074

(Figure 2). Here, the fluorescently labeled imidazoles and corresponding Co(III) Schiff base complex were used to design and evaluate the stability of imidazole-containing Co(III) complexes in the presence of competing small molecule ligands and peptides.

Guided by the fluorescent Co(III) complexes, a new dinuclear Co(III) complex with diimidazole axial ligands was prepared and characterized (see the diimidazole ligand in Figure 1C). Multidentate ligands have been extensively used to enhance the stability of coordination complexes.[23−27] Dissociation of such ligands at one coordination site does not predicate ligand exchange, since diffusion of the ligand is limited by coordination at one or more other sites at the metal center. As such, the diimidazole ligand in the dinuclear Co(III) complex was expected to retain a high local concentration at the Co(III) center, enabling rapid re-coordination and overall enhanced complex stability.[23,24] Not surprisingly, the dinuclear complex exhibited a 2-fold enhancement in stability to ligand exchange at neutral pH, compared to complexes with monodentate imidazole ligands, as well as resistance to hydrolysis at a biologically relevant pH range (<10% hydrolysis at pH ≥5). The properties of the dinuclear Co(III) complex provide insight into the design of a substitutionally inert axial ligands for incorporation into Co(III) Schiff base complex.

RESULTS

Design, Synthesis, and Characterization of a Fluorescent Imidazole and Its Co(III) Complex. A fluorescently labeled imidazole was synthesized for the analysis of axial ligand exchange. A coumarin-3-carboxylic acid core was attached to the 4-carbon position of the imidazole ring to produce the target ligand, C3Im (see Figure 1C, as well as SI Scheme 1 in the Supporting Information). The corresponding $[Co(acacen)(L)_2]^+$ complex, CoC3Im, was prepared using modified literature procedures (SI Scheme 1). C3Im exhibits fluorescence with the expected excitation/emission values (334 nm/410 nm; see SI Figure 1 (red traces) in the Supporting Information).[28] C3Im emission is quenched ∼8-fold in the corresponding Co(III) complex, CoC3Im (blue traces in SI Figure 1).

Previous work has utilized NMR with varying pH to evaluate the ligand dissociation of Co(III) Schiff base complexes.[15] To determine if ligand coordination can be measured by the fluorescence of C3Im, the emission and NMR spectra of CoC3Im were acquired at varying pH (or pD for NMR) (see Supporting Discussion 1 and SI Figures 2−5 in the Supporting Information). To quantify pH-dependent changes in emission intensity at the $\lambda_{F,max}$ (ex/em = 334/410 nm), alkaline solutions of CoC3Im and C3Im (50 and 100 μM, respectively; 20 mM phosphate buffer at pH 8.5, 2% methanol) were incubated with varying amounts of HCl for 1 h at 37 °C. The pH of the solutions were measured after spectra acquisition. For NMR studies, deuterated methanolic solutions of C3Im (5 mM) and CoC3Im (10 mM) were diluted by a factor of five with deuterated aqueous phosphate buffer at pH 8.5 containing an internal standard (DSS). DCl was titrated into each sample at varying increments. After each addition, samples were incubated for 30−60 min at 37 °C, then NMR spectra were acquired. The pD of the solutions were measured after spectra acquisition. The pD value at which 50% of CoC3Im undergoes hydrolysis was observed to occur at pD 5.2 (see Supporting Discussion 1 and SI Figure 5 in the Supporting Information).

An increase in the emission intensity of CoC3Im is observed with decreasing pH in a sigmoidal fashion (SI Figures 2 and 3). The midpoint of the pH-dependent emission occurs at pH 5.2, which is in excellent agreement with the pD value at which 50% of CoC3Im undergoes hydrolysis (as measured by NMR). Therefore, the observed pH-dependent increase in emission intensity of CoC3Im correlates to ligand dissociation, establishing CoC3Im and C3Im as valid tools for studying ligand exchange of imidazole-containing Co(III) Schiff base complexes by fluorescence.

Assessing Ligand Exchange Dynamics with C3Im and CoC3Im. Since the coumarin-derived fluorescence of C3Im is sensitive to Co(III) coordination, changes in the emission intensity of CoC3Im in the presence of competing ligands were used to assess the stability of previously investigated $[Co(acacen)(L)_2]^+$ complexes.[15,16] Ligand exchange of CoC3Im was evaluated in the presence of competing imidazole ligands, 2-methylimidazole (2MeIm), 4MeIm, NMeIm, and Im, as well as pyridine (Py) and ammonia (NH_3) (see Figure 3A).

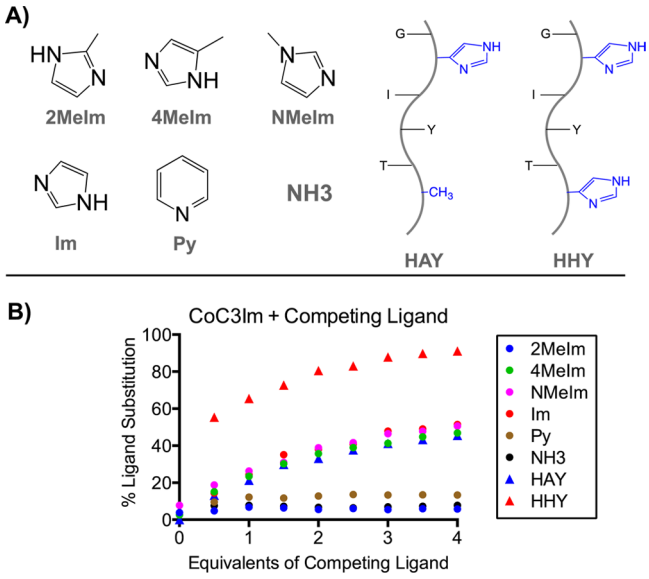

Figure 3. Ligand substitution of CoC3Im in the presence of competing ligands. Solutions of CoC3Im were combined with varying molar equivalents of nonfluorescent ligands (0.0−4.0 equiv) with a final concentration of 50 μM CoC3Im (20 mM phosphate buffer at pH 7.4, 2% methanol) and incubated for 1 h at 37 °C. The competing ligands are defined in panel A. Panel B shows the percentage ligand substitution with increasing equivalents of the competing ligand as measured by fluorescence intensity (see standard curve in SI Figure 6 in the Supporting Information) after 1 h incubation at 37 °C (ex/em = 334/410 nm).

Coumarin-derived fluorescence of the various solutions was monitored and correlated to the concentration of free C3Im by a linear standard curve (SI Figure 6). The increase in free C3Im was plotted as the proportion of the C3Im that dissociates from the complex (percentage ligand substitution) at increasing equivalents of the competing ligands (Figure 3B). A single CoC3Im molecule contains two C3Im ligands at the axial position; thus, 50% ligand substitution correlates to an average dissociation of one axial ligand and 100% correlates to an average dissociation of both axial ligands. However, it should be noted that, in these experiments, the final products in solution

DOI: 10.1021/acs.inorgchem.5b01415
Inorg. Chem. 2015, 54, 9066−9074

at equilibrium were not isolated and characterized, and the resulting solution may consist of a mixture of species.

Solutions of CoC3Im were combined with varying molar equivalents of nonfluorescent ligands (0.0−4.0 equiv) and incubated for 1 h at 37 °C. The concentrations of the solutions of nonfluorescent imidazoles were normalized in terms of total imidazole concentration (i.e., solutions of HHY and diimidazole ligands were prepared at one-half of the molecular concentration of monodentate imidazoles and HAY to account for the presence of two imidazoles per molecule). Incubation of CoC3Im with 2MeIm, NH_3, and Py for 1 h at 37 °C does not result in any detectable ligand substitution. These results are consistent with previous NMR studies attributing less favored coordination of 2MeIm to steric interference of the C4 methyl of the imidazole and the lability of the latter two to pK_a of the free ligands.[15,16] Treatment of CoC3Im with 4MeIm, NMeIm, and Im at 37 °C for 1 h results in ligand substitution that increases with increasing molar equivalents of the competing ligand to the starting C3Im concentration, with ∼50% of C3Im dissociating at 4 equiv of the competing ligand. These observations correlate well with previous NMR studies where the formation of mixed axial ligand species rather than complete substitution was observed.[15] Agreement of these with previous NMR investigations validates the employment of C3Im fluorescence to assess axial ligand stability and CoC3Im as a valid model for imidazole-containing $[Co(acacen)(L)_2]^+$ complexes.

Having established the utility of CoC3Im for evaluating complex stability, its reactivity was evaluated in the presence of two peptides—Gly-His-Ile-Tyr-Thr-His-Gly (HHY) and Gly-His-Ile-Tyr-Thr-Ala-Gly (HAY)—to mimic more complex biological scenarios (Figure 3A). The HHY sequence is derived from a fragment of the Snail1 protein, a zinc finger TF that has been established as a target of $[Co(acacen)L_2]^+$ complexes.[7,8,14,29] The sequence was modified with a tyrosine residue (Tyr, Y) for accurate concentration measurements and end-capped with inert glycines (Gly, G). The HAY sequence mirrors that of HHY, with the exception of the second histidine (His, H), which is modified to an alanine (Ala, A). These two peptides were evaluated for ligand exchange with CoC3Im to assess the stability of monodentate imidazole axial ligands in the presence of competing biomolecules (Figure 3B).

The dissociation of C3Im from CoC3Im in the presence of HAY exhibited a similar dose dependence to competition with 4MeIm, confirming the latter as an appropriate model for the coordination of a single histidine within a peptide. Interestingly, incubation of CoC3Im with HHY resulted in an increase in C3Im dissociation. At 1−2 equiv of HHY (or 2−4 equiv of histidines) to CoC3Im, ∼65%−80% dissociation of C3Im was observed. Almost 100% dissociation was observed at higher equivalents, suggesting near-complete substitution of the C3Im ligands at the axial positions with HHY. The different reactivity of CoC3Im to HHY and HAY demonstrates a stronger coordination propensity of a system containing two coordinating imidazoles tethered by a peptide chain. These results support previous observations that CoIm can still coordinate to, and inhibit, enzymes such as α-thrombin that contain multiple histidines in the active site.

Synthesis and Characterization of Diimidazole Ligands. To evaluate the hypothesis that chelating ligands may confer increased stability to $[Co(acacen)(L)_2]^+$, two diimidazole ligands were synthesized: 1,4-diimidazoylbutane (DiIm4) and 1,10-diimidazoyldecane (DiIm10) (Figure 1C). Based on reported crystal structures of $[Co(acacen)(L)_2]^+$ complexes and metal complexes with diimidazole-type ligands, the 10-carbon linker of DiIm10 is expected be sufficiently long for bridging or chelating $[Co(acacen)(L)_2]^+$ complexes through axial coordination.[15,16,30] In contrast, the 4-carbon linker of DiIm4 is expected to be too short to coordinate $[Co(acacen)(L)_2]^+$ complexes in a similar manner without distortion of the octahedral geometry.[15,16]

The diimidazole ligands were synthesized according to modified literature procedures and characterized using nuclear magnetic resonance (NMR) and mass spectrometry (MS). DiIm10 and DiIm4 were subsequently analyzed for their effectiveness to exchange with C3Im in CoC3Im by fluorescence intensity measurements, as described for the monodentate imidazole ligands and peptide systems (Figure 4).

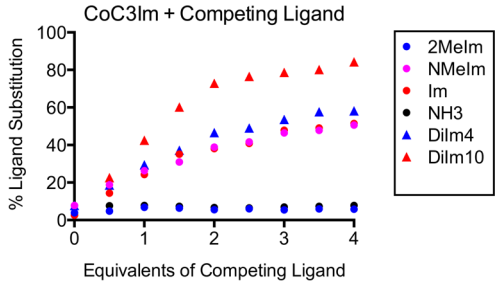

Figure 4. Ligand substitution of CoC3Im in the presence of diimidazoles (triangles). Solutions of CoC3Im were combined with 0.0−2.0 equiv of the diimidazole ligands with a final concentration of 50 μM CoC3Im (20 mM phosphate buffer at pH 7.4, 2% methanol) and incubated for 1 h at 37 °C. The *x*-axis corresponds to the equivalents of imidazole (i.e., solutions of the diimidazole ligands were prepared at one-half of the molecular concentration of monodentate imidazoles, to account for the presence of two imidazoles per molecule). Data for monodentate ligands 2MeIm, NMeIm, Im, and NH_3 have been reproduced from Figure 3B for comparison. Data are plotted as the percentage ligand substitution with increasing equivalents of the competing ligand, as measured by fluorescence intensity after 1 h of incubation at 37 °C (ex/em = 334/410 nm).

Incubation of CoC3Im with DiIm10 resulted in an increase in C3Im dissociation, relative to the monodentate imidazoles with dissociation values similar to those observed with HHY. At 1−2 equiv of DiIm10 (or 2−4 equiv of coordinating imidazoles) to CoC3Im, ∼70%−80% dissociation of C3Im was observed. In contrast, DiIm4 exhibited C3Im dissociation values that were almost identical to those of the monodentate ligand, as expected from the shorter carbon linker. These studies indicate that the chelating diimidazole ligand (DiIm10) may serve as a bidentate axial ligand with enhanced coordination stability in $[Co(acacen)(L)_2]^+$ complexes under normal physiological conditions.

Synthesis and Characterization of CoDiIm10. To evaluate the stability of DiIm10 as an axial ligand, a Co(III) Shiff base complex with DiIm10 axial ligands, termed CoDiIm10, was synthesized and its ligand exchange properties were analyzed (see Figure 1C and Figure 5). The electronic absorption spectrum of the isolated complex resembles $[Co(acacen)(L)_2]^+$ complexes (SI Figure 7 in the Supporting Information), suggesting that CoDiIm10 adopts an octahedral geometry with the tetradentate acacen ligand in the equatorial plane and N-donors at the axial positions. The ^1H NMR spectrum of CoDiIm10 shows a single species exhibiting chemical shifts corresponding to Co(III)-bound imidazoles,

DOI: 10.1021/acs.inorgchem.5b01415
Inorg. Chem. 2015, 54, 9066−9074

indicating that both imidazoles of DiIm10 are coordinating at the axial positions of the Co(III) complex (SI Figure 8). Peak integration suggests a 1:1 ratio between the acacen equatorial ligand and the diimidazole.

To determine the binding mode of DiIm10 in CoDiIm10, crystals of the product were grown and analyzed. The resulting crystal structure demonstrates a bridging (rather than chelating) binding mode of the DiIm10 (Figure 5). Bond

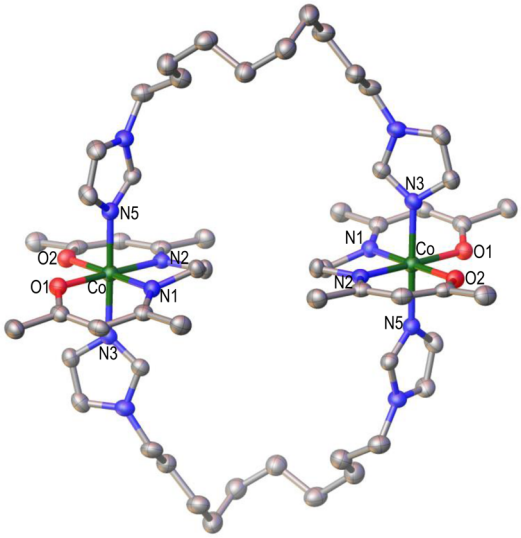

Figure 5. Molecular structure of CoDiIm10 (plot with 50% probability ellipsoids, cation only) shown with crystal structure labeling scheme. Select bond distances show no notable deviations in the Co−N bond distances, relative to the distances of $[Co(acacen)(L)_2]^+$ with imidazole axial ligands.

angles and distances were measured and compared to literature values for previously reported $[Co(acacen)(L)_2]^+$ complexes with monodentate axial ligands (Co4MeIm, CoNMeIm, and CoIm) (Table 1). One asymmetric unit is observed consisting of one $[Co(acacen)(L)_2]^+$ structure, or half of the molecule. To complete the molecule, two of these asymmetric units are joined in an antiparallel fashion. This results in a bridged complex containing an inversion center with diametrically opposite imidazoles exhibiting equivalent bond distances to the Co(III) center (Co−N3 and Co−N5; see Table 1 and Figure 5).

The asymmetric $[Co(acacen)(L)_2]^+$ unit exhibits conformations that are similar to the crystal structures of $[Co(acacen)(L)_2]^+$ complexes with monodentate imidazoles. The axial Co−N bond distances and bond angles in the equatorial acacen do not deviate from those observed in the structures of Co4MeIm, CoNMeIm, and CoIm. The similarities in structure indicate that the bridging binding mode of the DiIm10 does not result in a strain or distortion from the expected octahedral conformation.

Stability of CoDiIm10 to Hydrolysis. A sufficiently inert Co(III) Schiff base complex should be stable to hydrolysis in a biologically relevant pH range (pH 5.0−7.4) to prevent premature ligand dissocation in acidic environments such as the lysosome. To evaluate the stability of CoDiIm10 to hydrolysis under varying pH, the NMR spectra of DiIm10 and CoDiIm10 were acquired at varying pD (or apparent pH) values. Spectra were acquired under the same conditions as for C3Im and CoC3Im (see Supporting Discussion 1 in the

Table 1. Selected Bond Distances and Bond Angles for CoDiIm10 and $[Co(acacen)(L)_2]^+$ Derivatives (Where L = Monodentate Imidazoles)[a]

	Bond Distances (Å)			
	CoDiIm10	Co4MeIm[b]	CoNMeIm[c]	CoIm[b]
Co−O1	1.913	1.901	1.899	1.880
Co−O2	1.914	1.897	1.898	1.880
Co−N1	1.904	1.895	1.898	1.885
Co−N2	1.901	1.899	1.902	1.885
Co−N3	1.947	1.953	1.941	1.936
Co−N5	1.943	1.941	1.940	1.926
	Bond Angles (Deg)			
	CoDiIm10	Co4MeIm[b]	CoNMeIm[c]	CoIm[b]
O1−Co−O2	85.03	83.06	83.47	83.83
N1−Co−O1	94.90	95.69	94.79	95.29
N2−Co−O2	93.92	94.58	95.20	95.29
N1−Co−N2	86.15	86.75	86.58	85.60
N1−Co−N3	90.02	91.21	91.47	91.12
N2−Co−N3	89.11	90.99	89.16	91.12
O1−Co−N3	91.14	85.27	89.51	89.02
O2−Co−N3	90.78	89.96	90.41	89.02
N1−Co−N5	91.91	89.16	87.88	89.91
N2−Co−N5	90.05	91.81	91.08	89.91
O1−Co−N5	89.67	91.93	90.27	89.93
O2−Co−N5	87.28	89.61	90.23	89.93

[a]See complete data tables in SI Tables 1−7 in the Supporting Information. [b]Crystal structure reported in ref 13. [c]Crystal structure reported in ref 15.

Supporting Information; 80% D_2O buffered with 100 mM phosphate buffer, 20% MeOD; pD adjustment through DCl titration) to permit direct comparison.

To determine the pK_a of the diimidazole ligand, the chemical shift difference between the CH2 or CH5 protons of DiIm10 and an internal standard (DSS) were plotted as a function of the pD value of the solutions (SI Figure 9 in the Supporting Information). In addition, since alkylation of DiIm10 occurs at the N1 position, a CH4 proton could be monitored as well (~7.2 ppm at pH >8.0, SI Figure 9). From the midpoint of the resulting sigmoidal plot, the pK_a of the DiIm10 standard was determined to be 7.2. This pK_a value is within the same range as the value determined for C3Im (pK_a = 7.0) and the expected values of monodentate imidazoles.[31]

The pD-dependent behavior of CoDiIm10 was determined through analysis of the chemical shifts of the imidazole protons (Figure 6). Three major imidazole-containing species are observed by NMR as the pD of a solution of CoDiIm10 is varied: (1) the intact CoDiIm10, (2) a species in which one imidazole is coordinated to a Co(III) center and one is not (referred to as Mono-CoDiIm10 in Figure 6B), and (3) free DiIm10. Using the resolved peaks of the imidazole protons of these three species, the integrals of the species were plotted as a function of pD (Figure 6B).

Between pD 8.0 and pD 5.5, the solution primarily contains CoDiIm10, identified by its CH5 imidazole peak shifted upfield to 6.6 ppm. This is in contrast to CoC3Im, where dissociation is observed below pD ~6.5. As the value of pD is decreased below 5.5, the CH5 imidazole peak of CoDiIm10 decreases in intensity, while peaks corresponding to the CH2 imidazole proton of free DiIm10 (8.7 ppm) and the CH5 imidazole proton of Mono-CoDiIm (6.3 ppm) arise. As the value of pD is

DOI: 10.1021/acs.inorgchem.5b01415
Inorg. Chem. 2015, 54, 9066−9074

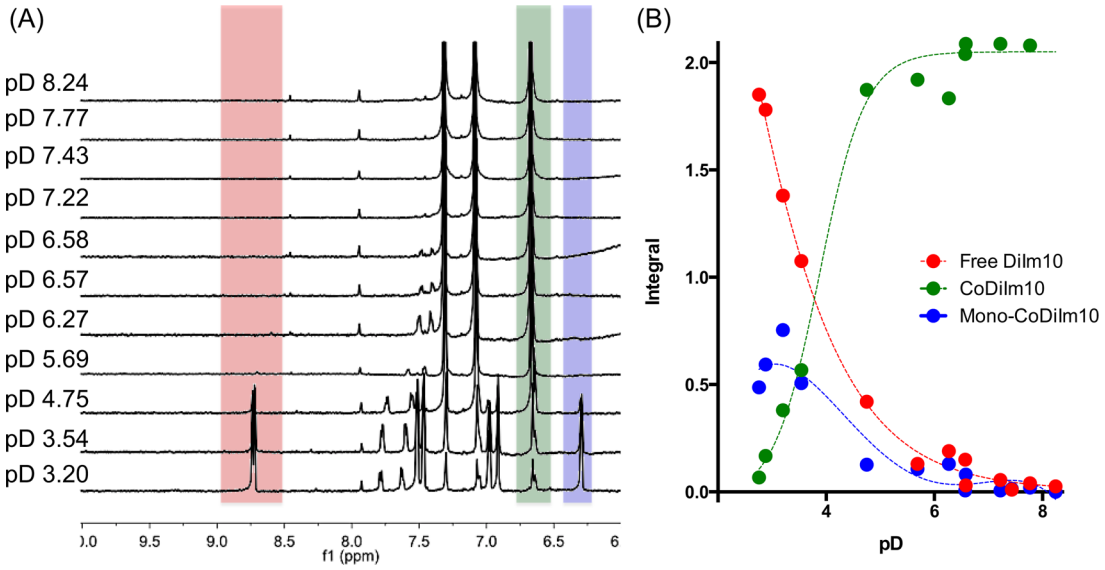

Figure 6. (A) NMR spectra of CoDiIm10 in deuterated methanolic solutions. CoDiIm10 (10 mM) was diluted by a factor of 5 with deuterated aqueous phosphate buffer at pH 8.5 containing an internal standard (DSS; final solution at 80% D_2O buffered with 100 mM phosphate buffer, 20% MeOD). DCl was titrated into each sample at varying increments. After each addition, samples were incubated for 30−60 min at 37 °C; then, NMR spectra were subsequently acquired. The pD of the solutions were measured after spectra acquisition. Peaks of interest are highlighted as follows; the CH2 peak of free DiIm (red), the CH5 peak of CoDiIm10 (green), and the CH5 peak of a species, where one imidazole of DiIm10 is Co(III)-bound and the other is consistent with a free imidazole (referred to as Mono-CoDiIm10 in panel B; blue). (B) Graph plotting the integrals of the imidazole protons of the three species as a function of pD for evaluating pD-dependent hydrolysis of CoC3Im. Nonlinear regressions (fourth-order polynomial fit for Free DiIm10 and Mono-CoDiIm10; sigmoidal fit for CoDiIm10) are fitted as dotted lines.

decreased below 3.0, the peaks corresponding to the Mono-DiIm species decrease while the free DiIm peaks continue to increase, progressing toward complete dissociation of DiIm10. The pD stability (the value of pD at which 50% of the CoDiIm10 remains) occurs at pD 3.9, more than 1 unit lower than the pD stabilities observed for $[Co(acacen)(L)_2]^+$ complexes with monodentate imidazoles, including CoC3Im (see SI Figure 5), indicating higher resistance of CoDiIm10 to hydrolysis.

Previous work had shown that pD stability of Co(III) Schiff base complexes deviate from pK_a trends of the free ligand in the presence of steric crowding from the axial ligand (as supported by decreased pD stability of $[Co(acacen)(2MeIm)_2]^+$). The behavior of CoDiIm shows that pD stability can be further tuned through modifying ligand denticity. Despite the similar pK_a values of DiIm10 to monodentate imidazoles, the bridging coordination mode confers enhanced hydrolytic stability to the complex at lower pD ranges.

Stability of CoDiIm10 to Ligand Exchange. The stability of CoDiIm10 to ligand exchange was evaluated in aqueous solutions through competition studies with free C3Im ligand and compared to Co2MeIm, Co4MeIm, CoNMeIm, CoIm, and $CoNH_3$ (Figure 7). Studies were performed with single-point fluorescence emission readings at the $\lambda_{F,max}$ (ex/em = 334/410 nm) of C3Im. Solutions containing either $[Co(acacen)(L)_2]^+$ complexes, CoDiIm10, or buffer alone (20 mM phosphate buffer, pH 7.4) were incubated with varying concentrations of C3Im at final concentrations of 50 μM (or 25 μM for CoDiIm10) and 0.0−4.0 equiv of C3Im, relative to cobalt content (20 mM phosphate buffer at pH 7.4, 2% methanol). The solutions were incubated for 1 h at 37 °C and fluorescent measurements were acquired. Displacement of the nonfluorescent axial ligands with C3Im were monitored by a loss in fluorescence intensity of C3Im that results from Co(III) coordination of the fluorescent ligand. Data points were plotted

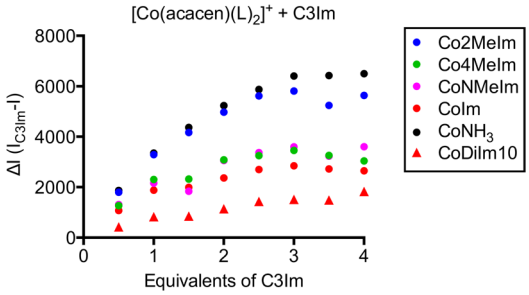

Figure 7. Competition of C3Im with CoDiIm10 and $[Co(acacen)(L)_2]^+$ complexes with monodentate axial ligands. Studies were performed with single-point fluorescence emission readings at the $\lambda_{F,max}$ (ex/em = 334/410 nm) of C3Im. Solutions containing either $[Co(acacen)(L)_2]^+$ complexes, CoDiIm10, or buffer alone (20 mM phosphate buffer, pH 7.4) were incubated with varying concentrations of C3Im with a final concentrations of 50 μM (or 25 μM for CoDiIm10) and 0.0−4.0 equiv of C3Im relative to cobalt content (20 mM phosphate buffer at pH 7.4, 2% methanol). The solutions were incubated for 1 h at 37 °C and fluorescent measurements were acquired. Stability to ligand exchange was monitored by loss in fluorescence of C3Im, and plotted in terms of ΔI values (ΔI = intensity of C3Im alone (I_{C3Im}) − intensity of C3Im incubated with Co(III) complexes (I)).

in terms of the difference in fluorescence intensity between the emissions of C3Im alone and C3Im incubated with the Co(III) complex (ΔI) at each concentration of C3Im evaluated. The ΔI values correspond to ligand exchange; thus, lower stability of a complex correlates to higher ΔI values.

For the previously studied $[Co(acacen)(L)_2]^+$ complexes, the following trend in ΔI values were observed: $CoNH_3 \approx$ Co2MeIm > Co4MeIm ≈ CoNMeIm > CoIm. Thus, the reverse trend was observed for complex stability. These relative stabilities are consistent with NMR spectroscopic investigations

DOI: 10.1021/acs.inorgchem.5b01415
Inorg. Chem. 2015, 54, 9066−9074

of the complexes, validating the use of ΔI values of C3Im competition studies to measure the stability of Co(III) Schiff base complexes to ligand exchange with competing imidazole ligands.[15]

In comparison to the previously studied complexes, CoDiIm10 exhibits a marked decrease in ΔI, demonstrating increased axial coordination stability conferred by the presence of a diimidazole ligand. The increased stability of CoDiIm10 is observed despite similarities in the bond lengths and angles of the crystal structures, compared to the complexes with monodentate imidazole ligand, thus attributing increased stability to the bridging binding mode. The behavior of CoDiIm10 suggests that axial ligands that bridge Co(III) centers to form multinuclear complexes may provide the stability necessary under normal physiological conditions to produce complexes that are activated only in the presence of an external trigger. These studies, combined with the C3Im competition studies, demonstrate the high stability of CoDiIm10 and its potential as a platform for activatable Co(III)-based protein inhibitors.

DISCUSSION

The axial ligand exchange investigations presented here provide design principles for activatable Co(III) Schiff base complexes. An imidazole equipped with a fluorescent coumarin core, C3Im, was synthesized and used to evaluate the axial ligand dynamics of imidazole-type ligands in $[Co(acacen)(L)_2]^+$ complexes. C3Im and the corresponding Co(III) complex, CoC3Im, were employed to evaluate the stability of monodentate imidazoles in the presence of competing peptides. The studies showed that, at neutral pH, monodentate imidazoles are readily displaced by a peptide containing two histidines, HHY, and thus such imidazoles do not provide sufficient stability as axial ligands for activatable Co(III) Schiff base complexes. This result is significant as several plasma proteins and target proteins, such as zinc finger TFs, contain multihistidine sites that can prematurely coordinate to $[Co(acacen)(L)_2]^+$ complexes (where L = monodentate imidazoles) prior to applying external triggers. Further photophysical characterization of coumarin-containing imidazole ligands will permit future quantification of axial ligand dynamics by fluorescence.

The fluorescent imidazole guided the design of a new Co(III) Schiff base complex with a diimidazole ligand, CoDiIm10, with increased stability. Crystal structure analysis revealed a bridging binding mode of DiIm10 at the axial positions of CoDiIm10, resulting in a dinuclear Co(III) Schiff base complex. CoDiIm10 exhibited resistance to hydrolysis at a biologically relevant pH range (apparent pH $\geq$5) and higher stability to C3Im competition, relative to the monodentate imidazole-containing complexes. Thus, in the design of activatable Co(III) complexes, diimidazole-containing molecules confer favorable stability under normal physiological conditions for controlled activation of Co(III)-based protein inhibitors.

The retention of the Co(III) octahedral conformation and axial ligand bond distances suggest that CoDiIm will be similarly activated by external triggers (e.g., light at 455 nm in the presence of a tethered Ru(II) bipyridal complex[19]) while remaining inert in the absence of the triggers. In addition, the differential behavior between bridging and monodentate ligands opens new opportunites for controlling ligand exchange. For example, the diimidazoles may be linked with a light harvesting unit to permit redox-activation by PET for increased spatial and temporal resolution. Alternatively, the bridging linker can be designed with peptide sequences that can be selectively cleaved by enzymes. Such a design would confer specificity of Co(III) complex activity for cancerous tissues if they are responsive to oncogenic enzymes (e.g., matrix metalloproteinases) or hypoxic conditions found in tumors.[32] Thus, these studies provide valuable principles for the design of biologically compatbile Co(III) Schiff base complexes as activatable protein inhibitors.

MATERIALS AND METHODS

Synthesis of C3Im. Coumarin-3-carboxylic acid (1.00 g, 5.26 mmol) was combined with *N*,*N*-dicyclohexylcarbodiimide (0.41 g, 15.78 mmol) and *N*-hydroxysuccinimide (1.82 g, 15.78 mmol) in 100 mL of dry DMF and stirred at room temperature for 2 h under N_2 atmosphere in darkness. Histamine dichloride (2.34 g, 21.04 mmol) and *N*,*N*-diisopropylethylamine in 5 mL of a solution containing 40% H_2O and 60% DMF was added to the coumarin reaction mixture and stirred overnight at room temperature under N_2 atmosphere in darkness. The reaction mixture was dried by rotary evaporation and then resuspended in HPLC-grade acetonitrile, and the white precipitate was removed by vacuum filtration. The filtrate was dried by rotary evaporation to produce a light yellow oil.

The crude oil was dissolved and purified by preparative HPLC using 0.05% TFA as the aqueous mobile phase and acetonitrile as the organic mobile phase with a linear gradient from 10% to 50% of the organic mobile phase over 20 min. The final product, C3Im, was dried by rotary evaporation, followed by lyophilization, to give a beige powder (yield of 52%). ^{1}H NMR (500 MHz, MeOD) δ: 8.89−8.83 (m, 2H), 7.87 (dd, J = 7.9, 1.5 Hz, 1H), 7.78 (ddd, J = 8.8, 7.4, 1.6 Hz, 1H), 7.51−7.42 (m, 3H), 3.77 (td, J = 6.7, 4.7 Hz, 2H), 3.08 (t, J = 6.7 Hz, 2H). ^{13}C NMR (126 MHz, MeOD) δ 162.71, 160.95, 154.51, 148.08, 134.27, 133.56, 131.40, 129.90, 125.15, 118.51, 118.09, 116.36, 116.08, 38.10, 24.33. High-resolution ESI-MS (positive mode): m/z = 284.1039 ($M + H^+$), 306.0852 ($M + Na^+$) (see SI Figure 10 in the Supporting Information).

Synthesis of CoC3Im. CoC3Im was synthesized according to modified literature procedures.[13,15] H_2(acacen) ligand was synthesized as described.[13,15] $CoBr_2{\cdot}6H_2O$ (14.4 mg, 44.0 μmol) and C3Im (50 mg, 176.0 μmol) were combined in 10 mL of methanol and stirred for 5 min under N_2. H_2(acacen) (10.9 mg, 48.4 μmol) that had been dissolved in 5 mL of methanol was added to the reaction mixture open to air to yield a pink solution. *N*,*N*-Diisopropylethylamine (DIEA, 60 μL, 352.0 μmol) was added directly to the reaction mixtures to yield a solution that had a royal blue color. The reaction was subjected to stirring for 16 h in an open-air environment to produce a brown solution.

The crude reaction mixture was dried by rotary evaporation, redissolved in minimum ethanol, and precipitated in diethyl ether. The final product, CoC3Im, was collected by vacuum filtration as a brown powder (33% yield). ^{1}H NMR (500 MHz, MeOD) δ: 8.88 (s, 2H), 7.90 (dd, J = 8.0, 1.5 Hz, 2H), 7.80 (ddd, J = 8.5, 7.2, 1.6 Hz, 2H), 7.53−7.45 (m, 4H), 7.33 (d, J = 1.4 Hz, 2H), 6.48 (d, J = 1.5 Hz, 2H), 4.98 (s, 2H), 3.64 (t, J = 6.5 Hz, 4H), 3.53 (s, 4H), 2.88 (t, J = 6.4 Hz, 2H), 2.20 (s, 6H), 2.01 (s, 6H). ^{13}C NMR (126 MHz, MeOD) δ: 177.90, 169.06, 162.25, 160.91, 154.46, 148.09, 136.56, 134.33, 129.96, 129.02, 125.24, 124.61, 118.52, 117.98, 116.07, 95.59, 52.33, 38.39, 24.37, 24.06, 21.04. High-resolution ESI-MS (positive mode): m/z = 847.2607 ($M^+ = [Co(acacen)(C3Im)_2]^+$), 564.1647 ($M^+ = [Co(acacen)(C3Im)]^+$) (see SI Figure 11 in the Supporting Information).

Synthesis of CoDiIm10. CoDiIm10 was synthesized according to modified literature procedures.[13,15] H_2(acacen) ligand was synthesized as described.[13,15] $CoBr_2{\cdot}6H_2O$ (22.6 mg, 69.1 μmol) and H_2(acacen) (17.0 mg, 76.0 μmol) were combined in methanol and stirred for 2 h under N_2 to produce a golden brown solution. DiIm10 (20.84 mg, 75.96 μmol) was added to the reaction mixture and stirred overnight in an open-air environment to produce a burnt orange solution. The reaction was dried by rotary evaporation to produce a green-brown oil.

DOI: 10.1021/acs.inorgchem.5b01415
Inorg. Chem. 2015, 54, 9066−9074

To purify CoDiIm10, the crude oil was redissolved in a minimum amount of ethanol and diluted with diethyl ether at room temperature to produce a brown solution with green-brown precipitate. The green-brown precipitate was separated from the ether/ethanol solution by centrifugation, and the supernatant was cooled to 4 °C for 18 h. The final product precipitated from the supernatant as a brown powder and was collected via vacuum filtration. The purification procedure was repeated three times with the green-brown precipitate from the first ether precipitation step.

The final product was collected as a brown powder (33% yield). (See the Crystal Structure Analysis of CoDiIm10 section below.) ^{1}H NMR (500 MHz, MeOD) δ: 7.41 (t, J = 1.4 Hz, 2H), 7.12 (t, J = 1.6 Hz, 2H), 6.69 (d, J = 1.7 Hz, 2H), 4.07 (t, J = 6.4 Hz, 4H), 5.12 (s, 2H), 3.62 (s, 4H), 2.29 (s, 6H), 2.09 (s, 6H), 1.51−0.96 (m, 16H). ^{13}C NMR (126 MHz, MeOD) δ: 177.86, 169.38, 138.27, 128.00, 120.32, 95.86, 52.37, 30.15, 29.12, 28.62, 25.65, 24.32, 21.19. ESI-MS (positive mode): m/z = 555.3 (M^{2+} = $[Co(acacen)(DiIm10)]_2^{2+}$), 829.3 ($M^{+}$ = $[Co(acacen)(DiIm10)_2]^{+}$), 1190.4 ($M^{+}$ = $([Co(acacen)(DiIm10)]_2Br)^{+}$), 275.2 (($M^{+}$ = DiIm10) + H^{+}). High-resolution ESI-MS (positive mode): m/z = 555.2851 (M^{2+} = $[Co(acacen)(DiIm10)]_2^{2+}$), 829.5017 ($M^{+}$ = $[Co(acacen)(DiIm10)_2]^{+}$), 1145.5387 ($M^{+}$ = $([Co(acacen)(DiIm10)]_2Cl)^{+}$) (see SI Figure 12 in the Supporting Information).

Ligand Competition Studies. *CoC3Im + Nonfluorescent Ligands.* Competition studies evaluating exchange between CoC3Im and nonfluorescent ligands were performed with single-point fluorescence emission readings on a Biotek Synergy 4 microplate reader at the $\lambda_{F,max}$ (ex/em = 334/410 nm) of C3Im. In a typical experiment, solutions of CoC3Im were combined with varying molar equivalents of nonfluorescent ligands (0.0−4.0 equiv) in 96-well plates to achieve a final concentration of 50 μM CoC3Im with a total volume of 100 μL per sample (20 mM phosphate buffer at pH 7.4, 2% methanol). The 96-well plate was incubated for 1 h at 37 °C. The concentrations of the solutions of nonfluorescent imidazoles were normalized in terms of total imidazole concentration (i.e., solutions of HHY and diimidazole ligands were prepared at one-half of the molecular concentration of monodentate imidazoles and HAY to account for the presence of two imidazoles per molecule). For standard curves, C3Im solutions were prepared at 20, 40, 60, 80, and 100 μM and plated in 96-well plates in triplicate for each experiment. Solutions of both CoC3Im and competing ligands and the C3Im standard solutions were incubated for 1 h at 37 °C.

Fluorescent measurements were acquired (ex/em = 334/410 nm) using autosensitivity settings with high emission wells normalized to 100 μM solutions of C3Im (set to 10000 a.u.). Each emission intensity value was converted to a percentage increase from CoC3Im values with 0.0 equiv competing ligands (percentage increase = $100 \times [(I - I_{CoC3Im,\,0\,equiv})/I_{CoC3Im,\,0\,equiv}]$). A standard curve was produced by plotting emission intensity vs [C3Im] and the data points were fit to a linear regression. The slope (m) and y-intercept (b) of the standard curve was used to determine the concentration of C3Im dissociated from Co3Im by ligand exchange for each nonfluorescent ligand ($[C3Im]_{dissoc}$ = [(percentage increase − b)/m]). Since the total [C3Im] in 50 μM of CoC3Im is 100 μM, $[C3Im]_{dissoc}$ for these experiments are equivalent to the percentage ligand substitution of C3Im. Ligand exchange propensities were compared by plotting the percentage ligand substitution versus equivalents of the competing ligand to CoC3Im.

Nonfluorescent Cobalt Complexes + C3Im Ligands. Competition studies evaluating exchange between CoC3Im and nonfluorescent ligands were performed with single-point fluorescence emission readings on a Biotek Synergy 4 microplate reader at the $\lambda_{F,max}$ (ex/em = 334/410 nm) of C3Im. Solutions containing either $[Co(acacen)(L)_2]^{+}$ complexes, CoDiIm10, or buffer alone (20 mM phosphate buffer, pH 7.4) were incubated with varying concentrations of C3Im to achieve final concentrations of 50 μM (or 25 μM for CoDiIm10) and 0.0−4.0 equiv of C3Im, relative to cobalt content (20 mM phosphate buffer at pH 7.4, 2% methanol). One hundred microliters (100 μL) of each sample were added to 96-well plates. The solutions were incubated for 1 h at 37 °C and fluorescent measurements were acquired using autosensitivity settings with high emission wells normalized to the highest concentration of C3Im incubated with buffer alone (set to 10000 a.u.). For each Co(III) complex, emission intensity values (I) were subtracted from the intensity values of C3Im at the same concentration incubated with buffer alone (I_{C3Im}). The stability of each complex to ligand exchange was evaluated with a plot of ΔI versus equivalents of C3Im, where $\Delta I = I_{C3Im} - I$.

Crystal Structure Analysis of CoDiIm10. Single crystals of $C_{56}H_{88}Br_2Co_2N_{12}O_4$ (CoDiIm10) were obtained by vapor diffusion of ether into ethanol. A suitable crystal was selected and mounted in inert oil and transferred to the cold gas stream of a Bruker Kappa APEX CCD area detector diffractometer. The crystal was kept at 99.96 K during data collection. Using Olex2,[33] the structure was solved with the XM[34] structure solution program, using Dual Space, and refined with the XL[34] refinement package using least-squares minimization.

Crystal data for $C_{56}H_{88}Br_2Co_2N_{12}O_4$ (M = 1271.06): monoclinic, space group $P2_1/c$ (No. 14), a = 14.0820(6) Å, b = 23.4788(10) Å, c = 9.2804(4) Å, β = 109.007(3)°, V = 2901.1(2) Å^3, Z = 2, T = 99.96 K, μ(Cu Kα) = 6.534 mm^{-1}, D_{calc} = 1.455 g/mm^3, 13 777 measured reflections (6.638° ≤ 2θ ≤ 131.95°), 4811 unique reflections (R_{int} = 0.0563, R_{sigma} = 0.0652), which were used in all calculations. The final R_1 was 0.0465 ($I > 2\sigma(I)$) and wR_2 was 0.1161 (all data). No special restraints or constraints were used in this refinement.

■ ASSOCIATED CONTENT

Supporting Information

The Supporting Information is available free of charge on the ACS Publications website at DOI: 10.1021/acs.inorgchem.5b01415.

Supporting discussion on pH-dependent behavior, synthesis of diimidazole ligands, high-resolution mass spectrometry spectra, pH-dependent fluorescence and NMR spectra, electronic absorption spectroscopy, crystal structure parameters, and additional experimental procedures (PDF)

Crystallographic information for $C_{56}H_{88}Co_2Ni_2O_4$ and $C_{56}H_{88}Br_2Co_2Ni_{12}O_4$ (CIF)

■ AUTHOR INFORMATION

Corresponding Author

*E-mail: tmeade@northwestern.edu.

Author Contributions

†These authors contributed equally to this work.

Notes

The authors declare no competing financial interest.

■ ACKNOWLEDGMENTS

The authors thank Dr. Natsuho Yamamoto and Dr. Robert Holbrook for helpful discussions. M.C.H. would like to acknowledge the National Science Foundation Graduate Research Fellowship. V.R. and J.L.C. would like to acknowledge a Northwestern University Undergraduate Research Grant from the Weinberg College of Arts and Sciences. V.R. further acknowledges the Northwestern University Chemistry of Life Processes Summer Fellowship. A.S.H. would like to acknowledge the Natural Sciences and Engineering Research Council of Canada graduate fellowship. E.A.B. acknowledges the National Institutes of Health, under Ruth L. Kirschstein National Research Service Award No. 1F31CA186761-01. This investigation was supported by the National Institutes of Health−National Institute of Arthritis and Musculoskeletal and Skin Diseases, under Award No. P30AR057216, and the National Institutes of Health, under Award No. R03CA167715.

DOI: 10.1021/acs.inorgchem.5b01415
Inorg. Chem. 2015, 54, 9066−9074

REFERENCES

(1) Casini, A.; Hartinger, C.; Gabbiani, C.; Mini, E.; Dyson, P. J.; Keppler, B. K.; Messori, L. *J. Inorg. Biochem.* **2008**, *102*, 564.
(2) Louie, A. Y.; Meade, T. J. *Chem. Rev.* **1999**, *99*, 2711.
(3) Che, C.-M.; Siu, F.-M. *Curr. Opin. Chem. Biol.* **2010**, *14*, 255.
(4) Bruijnincx, P. C.; Sadler, P. J. *Curr. Opin. Chem. Biol.* **2008**, *12*, 197.
(5) Meggers, E. *Chem. Commun. (Cambridge, U.K.)* **2009**, 1001.
(6) Prakash, J.; Kodanko, J. J. *Curr. Opin. Chem. Biol.* **2013**, *17*, 197.
(7) Harney, A. S.; Lee, J.; Manus, L. M.; Wang, P. J.; Ballweg, D. M.; LaBonne, C.; Meade, T. J. *Proc. Natl. Acad. Sci. U. S. A.* **2009**, *106*, 13667.
(8) Harney, A. S.; Meade, T. J.; LaBonne, C. *PLoS One* **2012**, *7*, e32318.
(9) Harney, A. S.; Sole, L. B.; Meade, T. J. *JBIC, J. Biol. Inorg. Chem.* **2012**, *17*, 853.
(10) Hurtado, R. R.; Harney, A. S.; Heffern, M. C.; Holbrook, R. J.; Holmgren, R. A.; Meade, T. J. *Mol. Pharmaceutics* **2012**, *9*, 325.
(11) Louie, A. Y.; Meade, T. J. *Proc. Natl. Acad. Sci. U. S. A.* **1998**, *95*, 6663.
(12) Takeuchi, T.; Böttcher, A.; Quezada, C. M.; Meade, T. J.; Gray, H. B. *Bioorg. Med. Chem.* **1999**, *7*, 815.
(13) Böttcher, A.; Takeuchi, T.; Hardcastle, K. I.; Meade, T. J.; Gray, H. B.; Cwikel, D.; Kapon, M.; Dori, Z. *Inorg. Chem.* **1997**, *36*, 2498.
(14) Heffern, M. C.; Kurutz, J. W.; Meade, T. J. *Chem.—Eur. J.* **2013**, *19*, 17043.
(15) Manus, L. M.; Holbrook, R. J.; Atesin, T. A.; Heffern, M. C.; Harney, A. S.; Eckermann, A. L.; Meade, T. J. *Inorg. Chem.* **2013**, *52*, 1069.
(16) Matosziuk, L. M.; Holbrook, R. J.; Manus, L. M.; Heffern, M. C.; Ratner, M. A.; Meade, T. J. *Dalton Trans.* **2013**, *42*, 4002.
(17) Takeuchi, T.; Böttcher, A.; Quezada, C. M.; Simon, M. I.; Meade, T. J.; Gray, H. B. *J. Am. Chem. Soc.* **1998**, *120*, 8555.
(18) Peterson, M. D.; Holbrook, R. J.; Meade, T. J.; Weiss, E. A. *J. Am. Chem. Soc.* **2013**, *135*, 13162.
(19) Holbrook, R. J.; Weinberg, D. J.; Peterson, M. D.; Weiss, E. A.; Meade, T. J. *J. Am. Chem. Soc.* **2015**, *137*, 3379.
(20) Kim, B. J.; Hambley, T. W.; Bryce, N. S. *Chem. Sci.* **2011**, *2*, 2135.
(21) Yamamoto, N.; Danos, S.; Bonnitcha, P. D.; Failes, T. W.; New, E. J.; Hambley, T. W. *JBIC, J. Biol. Inorg. Chem.* **2008**, *13*, 861.
(22) Yamamoto, N.; Renfrew, A. K.; Kim, B. J.; Bryce, N. S.; Hambley, T. W. *J. Med. Chem.* **2012**, *55*, 11013.
(23) Irving, H.; Williams, R. *J. Chem. Soc.* **1953**, 3192.
(24) Hancock, R. D.; Martell, A. E. *Chem. Rev.* **1989**, *89*, 1875.
(25) Parajo, Y.; Malina, J.; Meistermann, I.; Clarkson, G. J.; Pascu, M.; Rodger, A.; Hannon, M. J.; Lincoln, P. *Dalton Trans.* **2009**, 4868.
(26) Pinkowicz, D.; Li, Z. Y.; Pietrzyk, P.; Rams, M. *Cryst. Growth Des.* **2014**, *14*, 4878.
(27) Do, L. H.; Lippard, S. J. *J. Am. Chem. Soc.* **2011**, *133*, 10568.
(28) Wagner, B. D. *Molecules* **2009**, *14*, 210.
(29) Mingot, J. M.; Vega, S.; Maestro, B.; Sanz, J. M.; Nieto, M. A. *J. Cell Sci.* **2009**, *122*, 1452.
(30) Andrew, R. E.; Chaplin, A. B. *Dalton Trans.* **2014**, *43*, 1413.
(31) Albert, A. *Heterocyclic Chemistry*; 2nd Edition; Athlone Press: London, 1968.
(32) Kratz, F.; Müller, I. A.; Ryppa, C.; Warnecke, A. *ChemMedChem* **2008**, *3*, 20.
(33) Dolomanov, O. V.; Bourhis, L. J.; Gildea, R. J.; Howard, J. A. K.; Puschmann, H. *J. Appl. Crystallogr.* **2009**, *42*, 339.
(34) Sheldrick, G. M. *Acta Crystallogr., Sect. A: Found. Crystallogr.* **2008**, *64*, 112.

DOI: 10.1021/acs.inorgchem.5b01415
Inorg. Chem. 2015, 54, 9066−9074